UCRL-JC-128879
PREPRINT

# Source Description and Sampling Techniques in PEREGRINE Monte Carlo Calculations of Dose Distributions for Radiation Oncology

**A. E. Schach von Wittenau, L. J. Cox, P. M. Bergstrom Jr., W. P. Chandler, C. L. Hartmann-Siantar, S. M. Hornstein**

**This paper was prepared for submittal to the Joint Russian American Conference on Computational Mathematics Albuquerque, NM September 2 - 5, 1997**

**October 31, 1997**

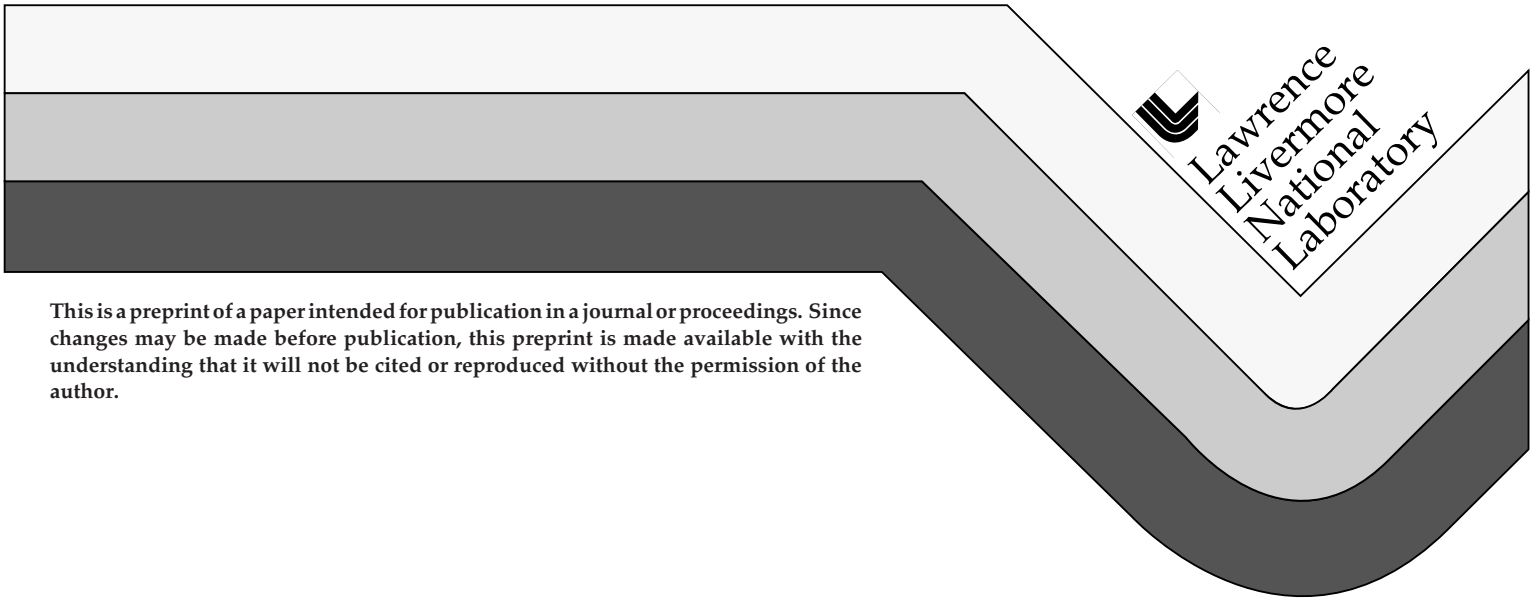

# Source Description and Sampling Techniques in PEREGRINE Monte Carlo Calculations of Dose Distributions for Radiation Oncology

A. E. Schach von Wittenau, L. J. Cox, P. M. Bergstrom Jr., W.P. Chandler, C.L. Hartmann-Siantar, and S. M. Hornstein

Lawrence Livermore National Laboratory, Livermore, CA 94550

## Abstract

We outline the techniques used within PEREGRINE, a 3D Monte Carlo code calculation system, to model the photon output from medical accelerators. We discuss the methods used to reduce the phase-space data to a form that is accurately and efficiently sampled.

## Introduction

PEREGRINE is a 3D Monte Carlo code calculation system designed specifically for radiation therapy planning. Unlike current dose calculation methods, which approximate dose distributions in the patient based on water phantom measurements, PEREGRINE determines the dose in the patient by simulating the actual treatment, particle interaction by particle interaction.

Accurate Monte Carlo dose calculations rely on a detailed understanding of the radiation source. One of the operational requirements for Monte Carlo treatment planning is that this detailed understanding be expressed as a set of distributions which may be rapidly and efficiently sampled, but which still accurately represent the underlying phase-space used to derive those distributions.

The nature of the problem is perhaps best understood in the context of Figure 1. A monoenergetic beam of electrons (~2 mm diameter) strikes a thin (~1 mm) target made of a high-Z material such as tungsten. The resulting bremsstrahlung photons are collimated by conical collimator (typically tungsten).

The photon beam passes through a beam flattener (also known as a flattening filter), which is usually made of Cu, Pb, or steel. The beam flattener, being thicker in the center, attenuates the central portion of the bremsstrahlung photon distribution. This results in a flat energy fluence distribution at the patient plane. Although the energy fluence distribution is uniform, the energy distribution itself is not uniform, since the photons landing at different points on the patient plane will have gone through differing thicknesses of the beam flattener. In addition, non-negligible amounts of radiation will scatter from the collimator and the beam flattener and arrive at the patient plane. This radiation field needs to be characterized by several distributions of bremsstrahlung and scattered photons

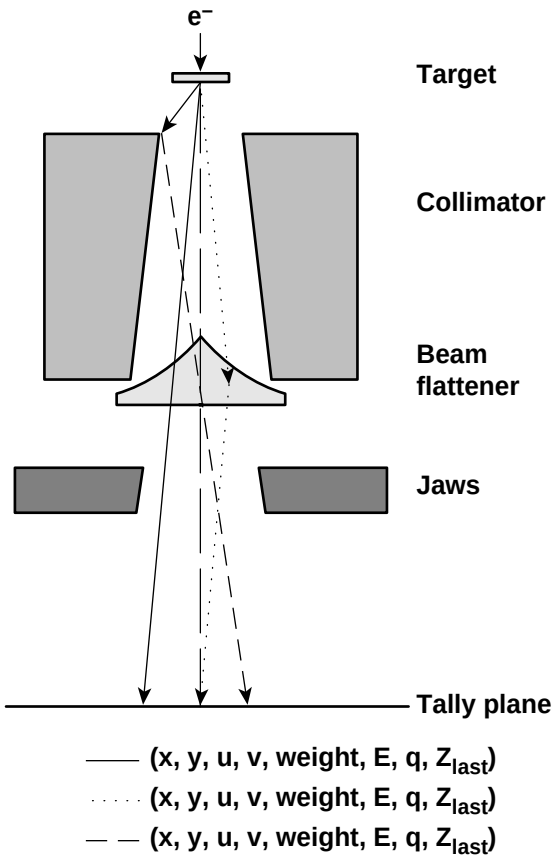


Figure 1: A stylized picture of the head portion of a medical accelerator. Monoenergetic electrons with energies of 4, 6, 8, 10, 15, or 18 MeV are incident on a thin (~1 mm), high-Z target such as tungsten. The bremsstrahlung radiation so produced is collimated by a primary collimator, also typically made from tungsten. The forward-peaked bremsstrahlung fluence distribution is 'flattened' by a conical piece of metal, typically made from copper. This filter, being thicker in the center, attenuates the center portion of the beam, primarily by attenuating the low energy portion of the photon distribution. Photons escaping the bottom of the accelerator head are tallied for later analysis.

*This work was performed under the auspices of the U.S. Department of Energy by the Lawrence Livermore National Laboratory under contract number W-7405-ENG-48.*

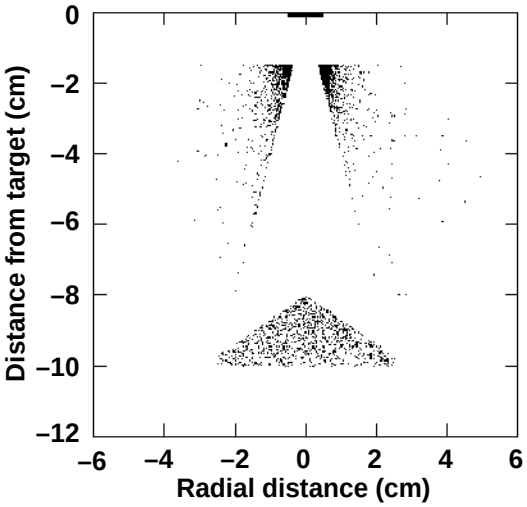


Figure 2. Backtracking the photons to their point of origin shows which portions of the accelerator head contribute to the output fluence.

and may be further shaped by beam shaping hardware such as movable jaws and other devices. All of these distributions must be understood in order to develop a useful source model for input into PEREGRINE. In addition, the source model derived from this understanding must satisfy the operational needs of being easily and efficiently sampled within the overall problem.

In this paper we present methods currently used within PEREGRINE to satisfy these requirements.

## Methods and Materials

The simulations were performed using the Monte Carlo codes BEAM96 [1] and MCNP4B [2]. Machine drawings and materials data for the medical accelerators discussed in this paper were supplied by Varian, Inc [3]. Both BEAM and MCNP have physics 'switches' which allow the biasing of the various physical processes that occur within the accelerator head. In addition, the BEAM code comes with the capability to record the 'position of last interaction' of a particle, as well as the number of the cell in which a given particle was created[1]. Only those portions of the treatment heads lying above the jaws were simulated, since this portion of the accelerator does not vary between treatments. Modeling of the movable jaws and patient-specific portions of the accelerator will be discussed elsewhere. A schematic of the modeling process is shown in Figure 1. The bremsstrahlung photons are tracked through the accelerator head. Photons arriving at the bottom of the head are tallied. Their position ***(x,y)***, their direction cosines ***(u,v)***, as well as their particle type, energy, weight (to account for the various physics-biasing schemes used), and position of last interaction $z_{last}$ are written to the phase-space file. The $z$ coordinate for each particle, being merely the tally-plane position, and the direction cosine $w$, known from

$$w = \sqrt{1-u^2-v^2}$$

do not need to be written to the file. Approximately $5\times10^6$ incident electrons are used in the simulations. Given the variance reduction schemes used (e.g., forced collisions, particle splitting), the resulting phase-space files contain information for several tens of millions of photons (of varying weights) and occupy ~1 GB of disk space each. To date we have simulated eight accelerators made by Varian, Inc. Work has started on accelerators made by Siemens, Inc.

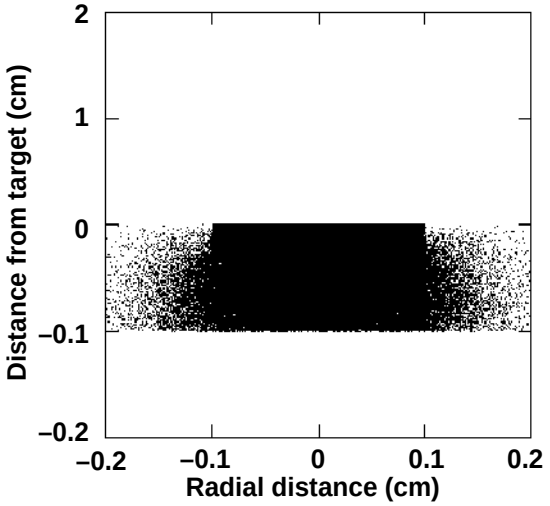


Figure 3. An expanded view of the region around the bremsstrahlung target of the stylized accelerator head shown in Figure 2. The sharp edges of the incident electron distribution are clearly visible, as is the broader, less intense distribution of photons that scatter within the target.

## Analysis of Phase Space Files

The first step in the analysis is to 'backtrack' the photons to their place of creation. This is done using the equations

$$x_s = x + (z_{last} - z_{tally}) \times u/w$$
$$y_s = y + (z_{last} - z_{tally}) \times v/w$$

A scatter plot of $x_s$ vs. $z_{last}$ for a stylized accelerator head is shown in Figure 2. This step in the phase-space analy-

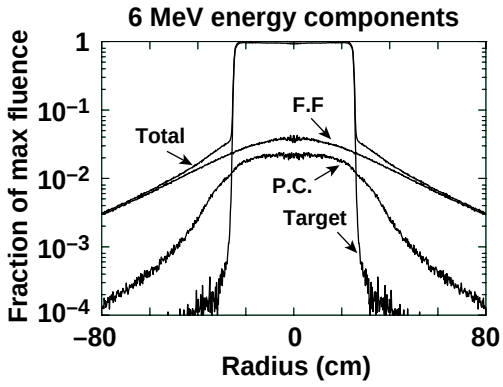


Figure 4. The fluence at the patient plane comprises contributions from the target, the primary collimator, and the flattening filter. The target is the major source of the energy reaching the patient.

1. We have since added this capability to MCNP, along with a number of other diagnostics which are not covered here.

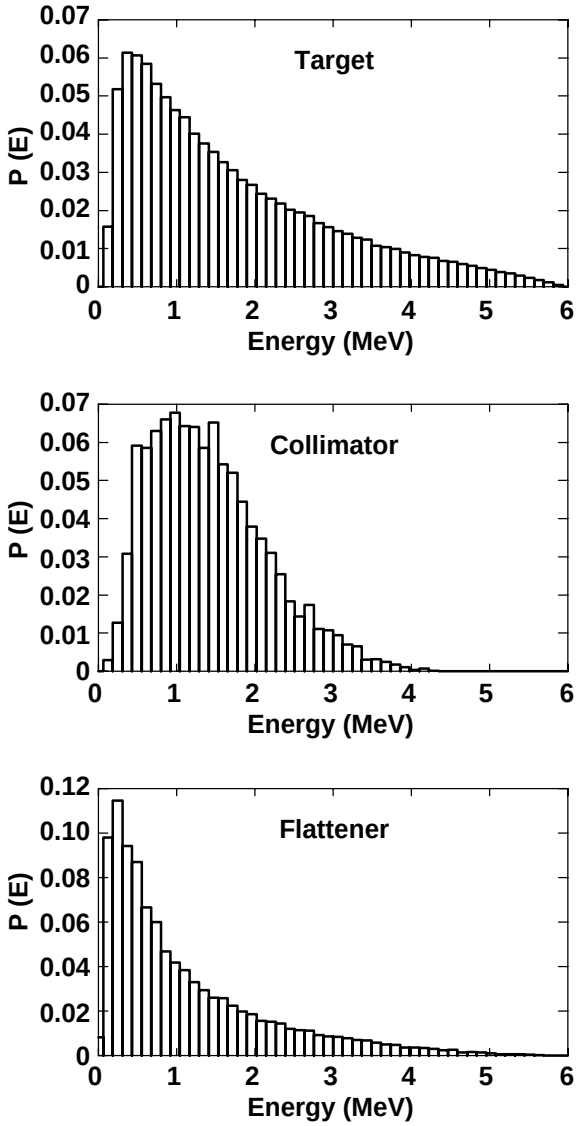


Figure 5. The photon energy distributions vary strongly with the piece of hardware in which they are created. Photons from the target have energies ranging from the energy of the initial electrons down to low, but not quite zero, energy. This is consistent with the flattening filter's removal of the lower energy photons. The energy distribution from the primary collimator reflects both this filtering process (on the low energy side) and the fact that the photons are Compton scattered through a non-negligible angle (thus affecting the high energy side). The photon distribution from the flattening filter reflects both the lack of low-energy filtering as well as the possibility for small angle scattering (and consequently little energy loss).

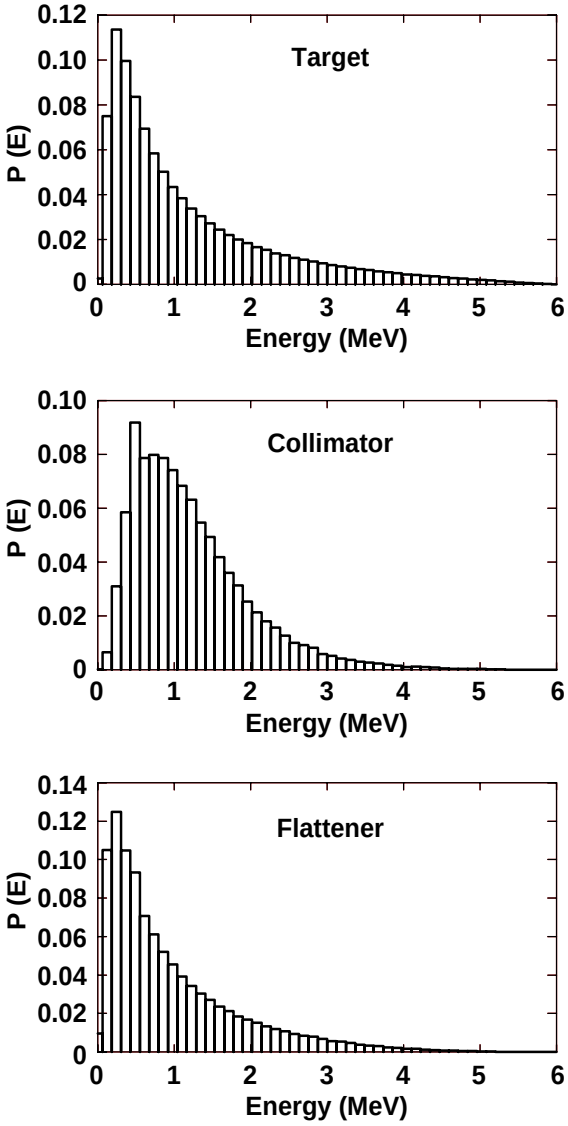


Figure 6. The photon energy distributions shown in Figure 5 change with increasing distance from the central axis of the accelerator. The energy distributions at a radius of 20 cm are shown.

sis serves two purposes — the first being practical, the second being conceptual. First, it is a useful check on the input deck, since the locations of the photon creations should correlate with the physical structure of the accelerator head. Second, it gives us a feel for how each portion of the hardware contributes to the output of the machine. For the example shown in Figures 2 and 3, we see that photons originating from the target come from a well defined spot. Photons coming from the primary collimator are fewer in number, and they tend to come from the upper edge of the collimator. Thus, the inner surface of the primary collimator is not a uniform source of photons. Rather, the primary collimator appears to be more of a 'ring' source. The flattening filter is also a source of photons. Unlike the primary collimator, however, the flattening filter is much more uniformly 'filled'.

We next analyze the fluence distributions at the patient plane. This is shown in Figure 4 for an accelerator operating at 6 MeV. We see that most of the energy comes directly from the target, with contributions at the several percent level from the flattening filter and the primary collimator.

### Energy Distribution

We show in Figure 5 the photon energy distributions from the various components at the center of the patient plane. The photon energy distributions vary strongly with the piece of hardware in which they are created. Photons from the target have energies ranging from the energy of the initial incident

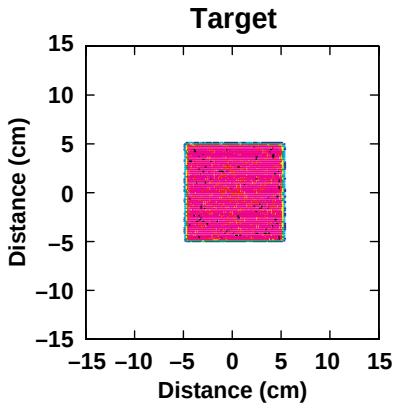


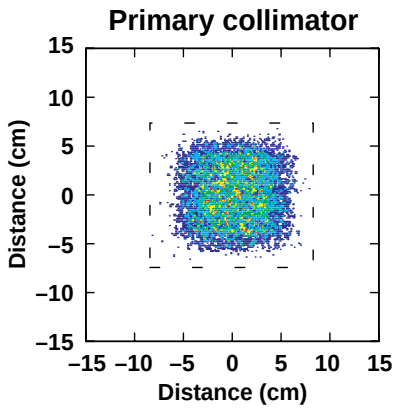


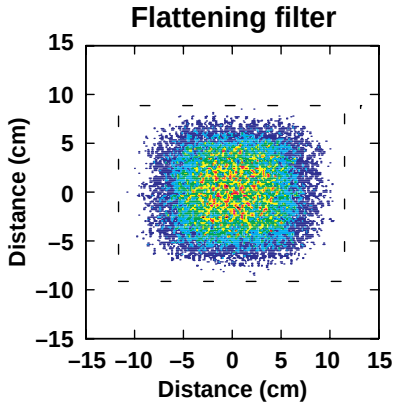


Figure 7. Each subsource illuminates a different amount of the patient surface. This area is a function both of the source 'size' as well as its distance to the jaws. The 'target' source is most sharply defined. The other sources illuminate larger areas of the patient. The dashed lines in the lower two panels denote a suitable area for Monte Carlo sampling.

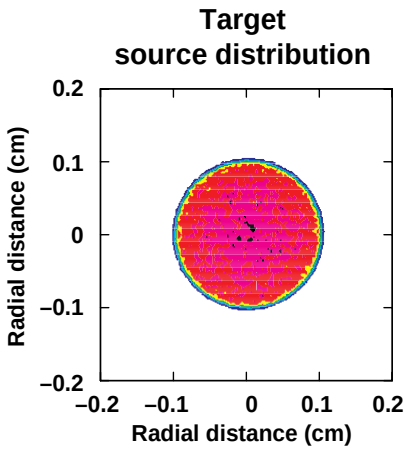


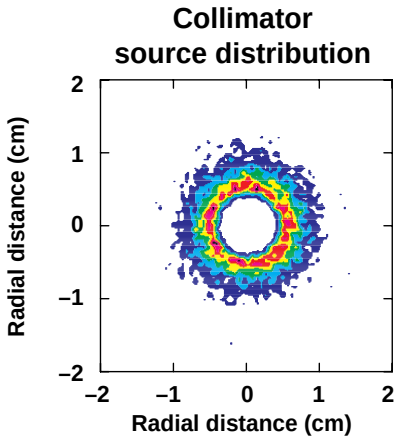


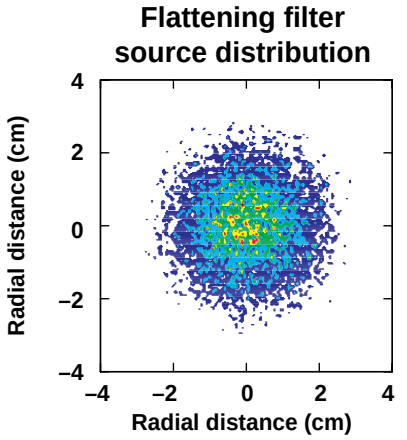


Figure 8. The effective source distributions, looking upwards from the patient plane towards the bremsstrahlung target. The photons coming from the target appear to come from a 2 mm diameter disk; those photons coming from the primary collimator appear to come from a ring-like source (compare with Figure 2); and those photons coming from the flattening filter appear to come from a broad, almost Gaussian-like source. Note the different diameters of the various sources.

electrons down to low, but not quite zero, energy. This is consistent with the flattening filter's removal of the lower energy photons. The energy distribution from the primary collimator reflects both this filtering process (on the low energy side) and the fact that the photons are Compton scattered through a non-negligible angle (thus setting an upper bound on the high energy side). The photon distribution from the flattening filter reflects both the lack of low-energy filtering (since this is the last piece of hardware transited by the photons) as well as the possibility for small-angle scattering (and consequently little energy loss) of the high energy photons coming from the target.

The energy distributions shown in Figure 5 change as we move to larger distances from the central axis of the beam. This is shown in Figure 6. We find that the distributions show an increase in the proportion of low energy (here, ~1 MeV) photons with increasing distance from the central axis, which correlates with the decrease in the thickness of the flattening filter traversed by these photons.

### Energy Fluence at Patient

The fluence patterns at the patient from each of the subsources for a 10 cm × 10 cm field (that is, where the jaws in Figure 1 have been moved so that the photons from the target illuminate a 10 cm × 10 cm square) are shown in Figure 7. We see that, as expected, the target photons illuminate the desired area. Photons from the primary collimator illuminate a larger area of the patient. This is expected, since the 'source' of these particular photons is both closer to the jaws and larger (Figure 2). This trend becomes even more pronounced for the photons from the flattening filter. Indeed, these photons illuminate a slightly rectangular area, a result of the different aspect ratio of the x- and y-jaw pairs. Analysis indicates that, at this field size, 93% of the photon energy reaching the patient comes from the target, 2% from the primary collimator, and 5% from the flattening filter.

While the area of illumination at a given field size is different for each subsource, it is true, on the other hand, that each subsource will illuminate a specific area of the patient for a specific jaw setting. The areas of illumination shown in Figure 7 can be studied for other jaw settings and the results tabulated for later use.

### Photon Origin Distribution

The subsources, in addition to illuminating different size areas of the patient, also have markedly different source distributions. Figure 8 shows the radial distribution of the photon energy for each subsource when the photons are backtracked to planes at positions corresponding to the locations shown in Figure 2. The 'target' photons source is a flat disk, the 'primary collimator' photons come from a ring-like source, and the 'flattening filter' photons come from a broad, almost Gaussian source. While these distributions are quite different, each is well described by a radial distribution and an angular distribution.

## Source Algorithm

We now have enough information to develop a source algorithm for use in PEREGRINE. The 'source' problem, as described in the Introduction, was to be able to generate photons in a manner that was both accurate and efficient. Let us consider the problem for a treatment consisting of one field size for one machine; the generalization to multiple field sizes is straightforward.

For a given field size, we know what proportion of the energy reaching the patient comes from each subsource (Figures 4 and 7).

Step 1: Decide which subsource will be sampled.

Step 2: For this subsource and field size, determine the ***x*** and ***y*** limits of illumination (Figure 7). Generate a random, uniformly distributed ***(x,y)*** coordinate within this area.

Step 3: Given this ***(x,y)*** pair, calculate ***r***. Adjust the weight of the particle to account for the slowly-varying fluence (Figure 4) of this subsource. Sample the particle's energy from the energy distribution for this subsource, at this ***r*** (Figures 5 and 6).

Step 4: Given the subsource being sampled, sample an initial position for the photon by choosing a starting radius and angle from the appropriate distribution (Figure 8).

At this point, we have the particle's energy and weight (Steps 2 and 3), as well as two points defining its trajectory (Steps 3 and 4). The trajectory-defining points define the particle's direction cosines, and we have all the required phase-space information needed to start tracking this particle in the patient. Sampling from the various distributions is performed using the alias sampling method [4]. 'Step 2' above keeps the efficiency of the overall algorithm high, since we tend to pick only those photons that will hit the patient.

## Conclusion

We have given an overview of the approaches used within the PEREGRINE project to model medical accelerators. We have described the variations in the energy and angular distributions of the radiation produced in or scattered by various portions of the accelerator. We have outlined our procedures for sampling these distributions to yield an algorithm that is both efficient and rapid.

## References

1. D.W.O. Rogers, B.A. Faddegon, G.X. Ding, C.-M. Ma, J. We, T.R. Mackie, Med. Phys., 22, 503 (1995).

2. J.F. Briesmeister, MCNP - A General Monte Carlo N-Particle Transport Code, LA-12625-M, Los Alamos National Laboratory (1997).

3. Varian Oncology Systems.

4. A.J. Walker, ACM Trans. Math. Software, 3, 253, (1977).

*Technical Information Department* • **Lawrence Livermore National Laboratory**
**University of California • Livermore, California 94551**